# A Study on ACO-OFDM Systems for Deep-Sea Visible Light Communications

Hiroshi Yamaoka[1] and Masato Saito[2]
[1]Graduate School of Science and Engineering, University of the Ryukyus
[2]Department of Electrical and Electronics Engineering, University of the Ryukyus
1 Senbaru, Nishihara, Okinawa 903–0213, Japan
E-mail : [1]k168529@eve.u-ryukyu.ac.jp, [2]masato_saito@m.ieice.org

**Abstract**: In this paper, we consider ACO-OFDM (Asymmetrically Clipped Optical-Orthogonal Frequency Division Multiplexing) based VLC (Visible Light Communication) systems for deep-sea communications. As the deep-sea channel model, we use the model which includes the effects of AWGN (Additive White Gaussian Noise) and attenuation due to water, chlorophyl, and fulvic and humic acid. We evaluate the ACO-OFDM system in terms of BER and average channel capacity.

## 1. Introduction

To explore submarine resources AUV (Autonomous Underwater Vehicle) is used [1]. For improving the exploring collaboration of multiple AUVs can be an efficient way and high-speed communications among AUVs are essential technologies. VLC (Visible Light Communication) attracts attention for communications methods in such deep-sea environment due to severe degradation of radio waves and relatively low data rate of acoustic waves [1].

To achieve high-speed VLC, several studies have been performed to apply OFDM (Orthogonal Frequency Division Multiplexing) systems to optical communication systems [3], [4], [2], [5].There are two ways to achieve optical OFDM systems, that is, DCO (DC biased Optical)-OFDM and ACO (Asymmetrically Clipped Optical)-OFDM [3]. In this study, we consider ACO-OFDM systems for sea-water optical communications due to relatively efficent use of signal power for communications [3]. In addition, we apply the attenuation model of sea water, which considers attenuation due to sea water and chlorophyl, to the evaluation of ACO-OFDM system [6]. According to the performance evaluations, efficient wavelength in terms of BER and channel capacity can change.

## 2. System Model

We consider ACO-OFDM systems for submarine or deep-sea communications systems. The system model is shown in Fig. 1. At the transmitter binary data sequences are input into the modulator to modulate the sequences to BPSK (Binary Phase Shift Keying) symbols. Then, the symbols are converted from serial to parallel sequences by S/P (serial-to-parallel) converter.

To generate ACO-OFDM signals, only odd number subcarriers are used to carry the symbols. Besides, IM/DD (Intensity-Modulated Direct-Detection) based schemes cannot treat neither complex nor negative signals. Therefore, first, Hermitian symmetry is used to generate real signals by IFFT (Inverse Fast Fourier Transform). The parallel input symbols $\mathbf{X}$ can be shown as

$$\mathbf{X} = \left[0, X_1, 0, X_3, \ldots, X_{\frac{N}{2}-1}, 0, X^*_{\frac{N}{2}-1}, \ldots, X^*_3, 0, X^*_1\right]^T, \tag{1}$$

where $N$ is the number of subcarriers including null subcarriers, $X_1, X_3, \ldots, X_{\frac{N}{2}-1}$ are data symbols, $X^*$ means complex conjugate of $X$, and $\mathbf{X}^T$ is the transpose of $\mathbf{X}$, respectively [3]. The complex conjugates are for the operation of Hermitian symmetry, that is, $X^*_k$ is carried at $N_f - k$-th subcarrier where $N_f$ is FFT (Fast Fourier Transform) point. The Hermitian symmetry can generate real OFDM signals. Since we consider ACO-OFDM systems, $X_k = 0$ for even number of $k$. Then, $n$-th sample of IFFT output sequences can be given as follows [3].

$$x_n = \frac{1}{\sqrt{N_f}} \sum_{k=0}^{N-1} X_k \exp\left(j\frac{2\pi nk}{N_f}\right) \tag{2}$$

Then, cyclic prefix is inserted into GI (Guard Interval). After P/S (Parallel-to-Serial) conversion, clipping the negative components of (2) generates ACO-OFDM signals $y_n$ [3]. The clipping function can be shown as

$$y_n = \begin{cases} x_n & x_n \geq 0 \\ 0 & x_n < 0 \end{cases} \tag{3}$$

The ACO-OFDM signal is converted from electrical to optical signals by LED and transmitted to sea water channel.

In the channel, we consider the effect of sea water on optical signals. The details are described in the next section.

At the receiver, APD (Avalanche PhotoDiode) receives the optical signals and converts the signals into the corresponding electical signals. The received signals are S/P converted. Then GI is removed, and the received signal without GI $r_n$ is input into FFT to recover the transmitted symbols. The $k$-th subcarrier of the FFT output $\hat{X}_k$ is shown as

$$\hat{X}_k = \frac{1}{\sqrt{N_f}} \sum_{n=0}^{N_f-1} r_n \exp\left(-j\frac{2\pi nk}{N_f}\right) \tag{4}$$

The demodulator demodulates the received signals and decides the transmitted symbols according to $\hat{X}_k$ for odd $k$ to recover the binary data sequence.

## 3. Sea water channel

In this section we describe and model the attenuation of optical signals due to the effect of sea water [6]. The intensity of light $I(\lambda)$ for wavelength $\lambda$ [nm] is shown as

$$I(\lambda) = I_0(\lambda) \exp\left(-d \cdot c(\xi, \lambda)\right), \tag{5}$$

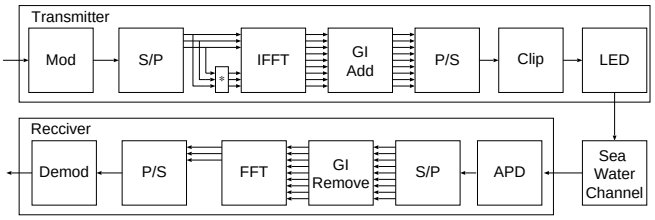


Figure 1. System model

where $\xi$ [$\mu$g/l] is the the density of chlorophyl, $c(\xi, \lambda)$ is an attenuation coefficient, $I_0(\lambda)$ is the incident intensity of light into water, and $d$ [m] is the distance between the transmitter and the receiver [1]. The attenuation coefficient can be shown as the sum of attenuation due to absorption $a(\xi, \lambda)$ and that due to diffusion $b(\xi, \lambda)$ [6], that is,

$$c(\xi, \lambda) = a(\xi, \lambda) + b(\xi, \lambda). \tag{6}$$

When we consider fulvic acid and humic acid as well as chlorophyl, the coefficient $a(\xi, \lambda)$ can be shown as

$$a(\xi, \lambda) = a_w(\lambda) + 0.06 a_C(\lambda) \xi^{0.602} + a_f C_f \exp(-k_f \lambda) + a_h C_h \exp(-k_h \lambda), \tag{7}$$

where $a_w(\lambda)$ and $a_C(\lambda)$ are the attenuation coefficient due to absorption by pure water and chlorophyl, respectively. $a_f$ and $a_h$ are the attenuation coefficients due to fulvic and humic acid, respectively. $k_f = 0.018$ [nm$^{-1}$] and $k_h = 0.01105$ [nm$^{-1}$] are constants relevant to fulvic and humic acid, respectively. $C_f$ and $C_h$ are the densities of fulvic and humic acid, respectively. These parameters are shown as

$$C_f = 1.74098 \xi \exp(0.12327 \xi) \tag{8}$$
$$C_h = 0.19334 \xi \exp(0.12343 \xi) \tag{9}$$

On the other hand, $b(\xi, \lambda)$ can be shown as

$$b(\xi, \lambda) = b_w(\lambda) + b_s(\lambda) C_s(\xi) + b_l(\lambda) C_l(\xi), \tag{10}$$

where $b_w(\lambda)$, $b_s(\lambda)$, and $b_l(\lambda)$ are attenuation coefficients due to diffusion by pure water, small particles, and large particles, respectively [6]. These parameters are given as

$$b_w(\lambda) = 0.005826 (400/\lambda)^{4.322} \tag{11}$$
$$b_s(\lambda) = 1.151302 (400/\lambda)^{1.7} \tag{12}$$
$$b_l(\lambda) = 0.341074 (400/\lambda)^{0.3} \tag{13}$$

$C_s(\xi)$ and $C_l(\xi)$ are the densities of small and large particles, respectively. These parameters are shown as

$$C_s = 0.01739 \xi \exp(0.11631 \xi) \tag{14}$$
$$C_l = 0.76284 \xi \exp(0.03092 \xi) \tag{15}$$

## 4. Numerical results

In this section, we evaluate the performance of ACO-OFDM systems through computer simulation. We use the parameters of ACO-OFDM systems tabulated in Table 1. Although the number of data subcarriers is 26, the number of active subcarriers, non-zero subcarriers, is $N = 52$. Besides, the FFT point is $N_f = 128$ which is the minimum number for ACO-OFDM system when $N = 52$ and the FFT point is $2^n$. In the following numerical evaluations, we use three colors of LED, that is, blue, green, and red. The correspoinding wavelength is shown for each color in Table 1.

Table 1. Simulation parameters

| Parameter | Value |
|---|---|
| The number of data subcarriers | 26 |
| The number of active subcarriers $N$ | 52 |
| FFT point $N_f$ | 128 |
| GI length | 32 |
| Modulation Scheme | BPSK |
| Wavelength of blue | 470 nm |
| Wavelength of green | 530 nm |
| Wavelength of red | 625 nm |

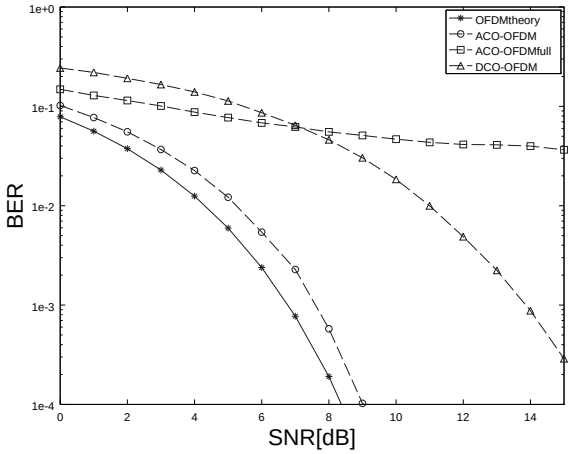


Figure 2. BER performances in AWGN channel

First, we show the BER (Bit Error Rate) performances versus SNR (Signal-to-Noise Ratio) of ACO-OFDM system as "ACO-OFDM", ACO-OFDM system which uses also even subcarriers as "ACO-OFDMfull", and DCO-OFDM systems as "DOC-OFDM" in Fig. 2. In the DCO-OFDM systems, each OFDM symbol is biased by the maximum amplitude in the negative region. Theoretical BER of complex OFDM signal is also plotted in the figure for comparison purpose as "OFDMTheory."

As we can see, ACO-OFDM achieves better BER performance than both DCO-OFDM and ACO-OFDM with full-subcarrier use. Since DCO-OFDM signal spends power for bias components, required SNR for BER of $10^{-3}$ is about 6 dB. As for ACO-OFDM signal with full-subcarrier use, even if the number of data subcarriers is doubled compared to normal ACO-OFDM systems, inter-carrier interference caused by clipping with such a dense subcarrier allocation significantly degrades the performances as shown in the figure.

We provide BER comparison between ACO-OFDM and DCO-OFDM systems in the sea water channel for $\xi = 0$ in

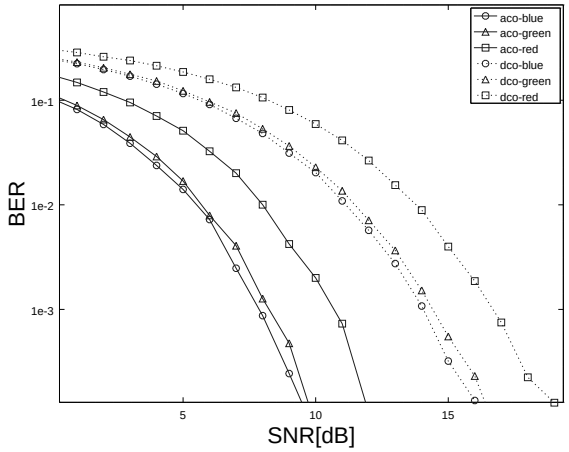


Figure 3. BER comparison between ACO-OFDM and DCO-OFDM systems in sea water channel

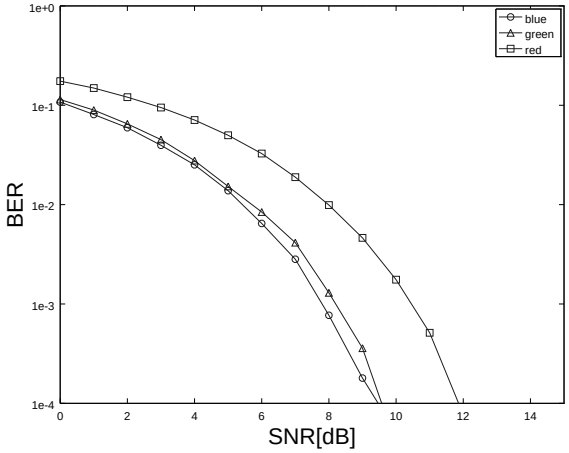


Figure 4. BER performances in sea water channel ($\xi = 0$).

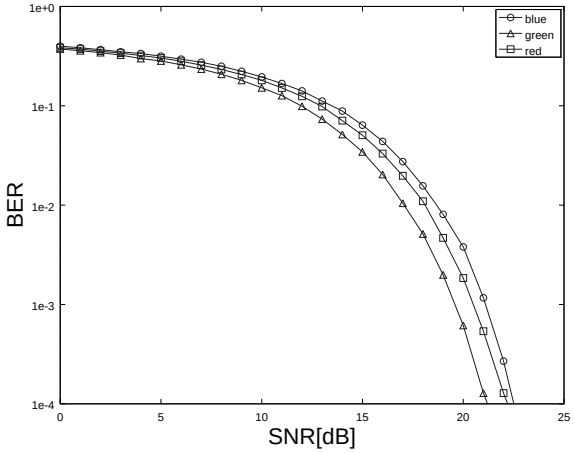


Figure 5. BER performances in sea water channel ($\xi = 4$).

Fig. 3. We use three wavelengths which correspond to the colors of blue, green, and red. As we can see in the figure, ACO-OFDM systems achieve about 6 dB better BER performances compared with DCO-OFDM systems for all colors. This performance differences are similar to those in AWGN channel.

We show BER performances of ACO-OFDM systems using three colors as a carrier in sea water channel with chlorophyl of $\xi = 0, 4$, and $8$ [$\mu$g/l] in Figs. 4, 5, and 6, respectively. Here, we assume the distance between the transmitter and the receiver $d = 1$ [m].

As we can see in Fig. 4, the BER performance of blue achieves the best in three when $\xi = 0$. However, the performance of green is close to the one of blue. On the other hand, BER performance of red degrades by 2 dB to achieve the BER of $10^{-3}$ compared with the others.

For $\xi = 4$, due to heavy attenuation by sea water and chlorophyl the BER performances of all colors severely degrades comppared with those in Fig. 4. The degradation can be confirmed Because the distance between the transmitter and receiver is the same as that in Fig. 4 and the density of chlorophyl increases. Among three colors, the BER of green can obtain approximately 1 dB gain to achieve BER of $10^{-3}$ in the case of $\xi = 4$.

When $\xi = 8$, the BER comparisons are shown in Fig. 6. As we can see, the BER performance of red requires minimum SNR to achieve the BER of $10^{-3}$ in this case. Therefore, the color or wavelength which achieves maximum gain can differ in the density $\xi$. However, due to the denser clorophyl, the required SNR to achieve the same BER the case of $\xi = 8$ needs approximately additional 35 dB compared with the case of $\xi = 0$.

## 5. Conclusion

In this study, we evaluate ACO-OFDM systems with different wavelengths in sea-water channel considering the density of chlorophyl. Through the BER evaluations, we find there exists appropriate wavelength of the optical signals for different density of chlorophyl. On the other hand, the denser the density of chlorophyl becomes in sea water, the more the BER performance degrades.

Since the performance evaluation has done in simple conditions, as the future work, we need to consider more realistic conditions such as the responses of LED and photodiode to electrical signals, the particular noise in optical devices other than AWGN. Also, the system treated in this study is simple, it is required to improve the SNR of the received signal by using coding of the transmitted symbols with Hermitian symmetry and appropriately combining the received symbols from two subcarriers. It is required to develop efficient channel estimation method suitable for the channel as well. Besides, to improve the SNR of the received signal it would be useful to apply power allocation method for ACO-OFDM signals in several wavelenths to maximize channel capacity of the system.

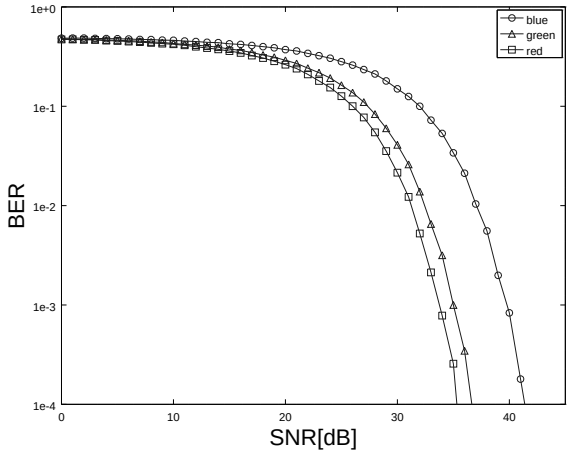


Figure 6. BER performances in sea water channel ($\xi = 8$).

## References


[1] X. Lin, "Wavelength-adaptation technique for LED-based underwater data communications using visible light," *JAMSTECRep. Res. Dev.*, vol. 19, pp. 11–18, Sep. 2014. doi: 10.5918/jamstecr.19.11

[2] H.M. Oubei, J.R. Duran, B. Janjua, H.Y. Wang, C.T. Chi, T.K. Ng, H.C. Kuo, J.H. He, M.S. Alouini, G.R. Lin, and B.S. Ooi, "4.8 Gbit/s 16-QAM-OFDM transmission based on compact 450-nm laser for underwater wireless optical communication," *Optics Express*, vol. 23, no. 18, pp. 23302–23309, Sep. 2015.

[3] Q. Wang, C. Qian, X. Guo, Z. Wang, D.G. Cunningham, and I.H. White, "Layered ACO-OFDM for intensity-modulated direct-detection optical wireless transmission," *Optics Express*, vol. 23, no. 9, pp. 12382–12393, May 2015. doi: 10.1364/OE.23.012382

[4] S. Haruyama, "Current Trends of Visible Light Gommunication," *J. Illum. Engng. Jpn.*, vol. 98, no. 10, pp. 538–541, Oct. 2014.

[5] J. Armstrong and B.J.C. Schmidt, "Comparison of Asymmetrically Clipped Optical OFDM and DC-Biased Optical OFDM in AWGN," *IEEE Commuun. Lett.*, vol. 12, no. 5, pp. 343–345, May 2008. doi: 10.1109/LCOMM.2008.080193

[6] T. Mori, Y. Kozawa, and Y. Umeda, "A Study of convolution coded OOK system using multi-color LED for high-speed underwater visible light communications," *IEICE Tech. Rep.*, vol. 115, no. 366, pp. 139–144, Dec. 2015.